

Observation of a blue shift in the optical response at the fundamental band gap in Ga_{1-x}Mn_xAsT. de Boer,¹ A. Gamouras,¹ S. March,¹ V. Novák,² and K. C. Hall¹¹*Department of Physics and Atmospheric Science, Dalhousie University, Halifax, Nova Scotia, Canada B3H 1Z9*²*Institute of Physics AS CR, Cukrovarnická 10, 162 53 Praha, Czech Republic*

(Received 17 November 2011; published 6 January 2012)

We report the observation of a sharp band-edge response in spectrally resolved differential reflectivity experiments on GaMnAs, in contrast to linear optical experiments in which large band-tail effects are known to dominate. The differential reflectivity response exhibits a blue shift relative to results in GaAs and LT-GaAs, consistent with the valence-band model of ferromagnetism. Our results demonstrate the utility of nonlinear optical techniques for studying the electronic structure of III-Mn-V diluted magnetic semiconductors.

DOI: [10.1103/PhysRevB.85.033202](https://doi.org/10.1103/PhysRevB.85.033202)

PACS number(s): 75.50.Pp, 71.20.Nr, 78.47.jg

Diluted magnetic semiconductors (DMSs), which result from doping traditional semiconductors with magnetic impurities, have been the subject of an intensive research effort in recent years due to their potential for applications in spin-sensitive electronics,¹⁻³ photonics,⁴⁻⁶ and optically-addressable nonvolatile memory.⁷⁻⁹ This potential stems from the hole-mediated nature of the ferromagnetic coupling between the local magnetic impurities, which permits external control of magnetic characteristics using electrical gates or optical excitation.¹⁰⁻¹³ GaMnAs has become the prototype DMS system, representing a model for understanding the nature of ferromagnetic coupling in the III-Mn-V DMS as well as for engineering the magnetic characteristics through tailored growth and processing.¹⁴⁻¹⁶ A considerable body of research spanning the past decade has provided insight into the nature of exchange coupling between the Mn and hole spins,¹⁷⁻²¹ the character of the magnetic anisotropy,²²⁻²⁵ and the role of defects and compensation in determining the magnetic characteristics.^{14,16,26,27}

Despite these advances, unanswered questions remain with regard to the electronic structure and the appropriate model of ferromagnetic coupling. An active debate in the recent literature has focused on the position of the Fermi level, in particular whether the holes that mediate ferromagnetic coupling between the local Mn moments exist in the GaAs valence band or in a detached impurity band.^{16,18,20,21,27-31} As the physical mechanism of ferromagnetic coupling differs in the two limits, determining the correct picture is of central importance. Considerable input into the debate has been provided through recent experiments, with evidence supporting both points of view.^{16-21,27,29}

Nonlinear optical spectroscopy provides an alternative approach to investigating the position of the Fermi level in GaMnAs. In pump-probe spectroscopy, a femtosecond optical pulse (pump pulse) is used to excite electron-hole pairs in the semiconductor. These carriers modify the optical response of a subsequent, weaker pulse (probe pulse), providing a way to detect the presence of the pump-injected carriers. If the Fermi level in GaMnAs exists in the valence band, one expects to observe a blue shift in the band-edge optical response relative to undoped GaAs (the so-called Moss-Burstein shift)³² since states that are full prior to the arrival of the pump pulse cannot lead to a signal. Alternatively, if the valence states are empty (with holes residing in a detached impurity band),

the pump-induced probe signal should experience an onset at or below the band gap of undoped GaAs.³³ In contrast to linear spectroscopy, in which strong band-tailing effects prevent the observation of any feature at the fundamental band gap,^{17,34-36} nonlinear spectroscopy is expected to provide a clear measurement of the band-gap energy, since the optical response associated with the band-tail states is expected to be diminished in the nonlinear regime.³⁷

Here we report results of spectrally resolved differential reflectivity measurements over a broad spectral range (1.4–2.0 eV) in GaMnAs. A sharp onset in the optical response is observed at the fundamental band gap, in contrast to linear absorption experiments, demonstrating the utility of nonlinear optical techniques for studying the electronic structure of the III-Mn-V DMS materials. Our findings indicate a clear blue shift of the band-edge response relative to undoped GaAs and low-temperature grown GaAs, providing support for the valence-band picture of ferromagnetism in GaMnAs.

Three samples were grown for this work. Each consists of a layer of Ga_{1-x}Mn_xAs (or GaAs) grown at low substrate temperature (195 °C) on top of a 220-nm GaAs buffer layer on a GaAs (001) substrate. One of the GaMnAs samples [with $x = 0.10$ and a ferromagnetic transition temperature (T_C) of 135 K] is 150 nm thick, and the other (with $x = 0.12$, $T_C = 183$ K) is 20 nm thick. Both GaMnAs samples were annealed in order to maximize T_C .¹⁶ A sample with $x = 0$ and a thickness of 150 nm (low-temperature-grown GaAs, LT-GaAs) was also grown. The optical response of the GaMnAs and LT-GaAs samples was compared to results from a semi-insulating GaAs substrate (SI-GaAs). The time-resolved differential reflectivity apparatus is shown in Fig. 1(a). The linearly polarized pump laser pulses have a center photon energy of 1.55 eV and a duration of 60 fs (bandwidth 58 meV). A femtosecond white light continuum was used as a broadband probe pulse.⁸ The change in the reflectivity of the probe pulse induced in the sample by the pump pulse (ΔR) was normalized to the unsaturated reflectivity (R_0), and measured as a function of probe-pulse delay and probe photon energy using a monochromator (resolution 9 meV) and lock-in detection techniques. The focal spot of the laser is 30 μm in diameter, and the estimated density of electron-hole pairs excited by the pump pulse is $4 \times 10^{19} \text{ cm}^{-3}$. For all experiments, the samples were cooled to 80 K at zero magnetic field.

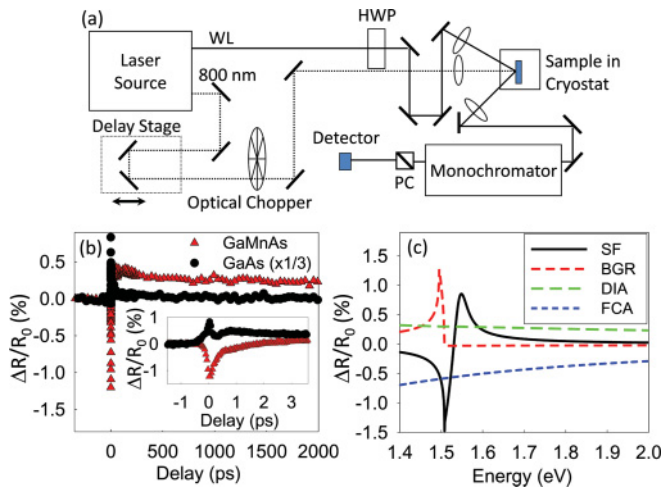


FIG. 1. (Color online) (a) Schematic diagram of the pump-probe apparatus. (b) Results of differential reflectivity experiments at a probe photon energy of 1.65 eV for SI GaAs (circles) and the 150-nm-thick GaMnAs sample (triangles). (c) Results of model calculations of differential reflectivity spectra using an effective mass model and a thermalized carrier distribution with a temperature of 80 K, separating contributions due to SF, BGR, FCA, and DIA. For the BGR curve, a small band edge shift of 13 meV was introduced by hand following Ref. 38. For DIA, $\Delta\alpha$ was assumed to be proportional to the conduction-band density of states with an onset of absorption from the $A_{S_{Ga}}$ band at half the band-gap energy.

The differential reflectivity results at a probe energy of 1.65 eV for SI-GaAs and the 150-nm GaMnAs sample are shown in Fig. 1(b). The evolution of $\Delta R/R_0$ with probe-pulse delay differs considerably for these two samples. For SI-GaAs, the signal is positive for all time delays and decays to nearly zero within the first 50 ps. In contrast, the $\Delta R/R_0$ signal in GaMnAs is initially negative, and subsequently changes sign, producing a large positive signal on long time scales. A broader view of the differential reflectivity response in these two samples is provided in Figs. 2(a) and 2(b), where the measured signal is plotted over a wide range of probe photon energies. After the initial fast relaxation dynamics, the $\Delta R/R_0$ signal in SI-GaAs is concentrated near the band gap, where it slowly decays with probe-pulse delay. The nonlinear response in GaMnAs, in contrast, consists of a broad positive feature with a sharp onset at 1.562 eV. Weak features also exist in the data in Fig. 2(b) at the band gap of SI-GaAs and at the pump-pulse excitation energy (1.55 eV).

In SI-GaAs, the carrier dynamics following excitation by a femtosecond laser pulse are well understood,³⁹ consisting of an initial rapid thermalization process that results in a Fermi distribution with an elevated temperature, followed by carrier cooling and ultimately recombination with the optically excited holes in the valence band. The carrier dynamics are modified in GaMnAs by the presence of a large density of $A_{S_{Ga}}$ defects, which form a mid-gap donor band and lead to rapid trapping of electrons out of the conduction band on a time scale of a few picoseconds or less.^{8,40–47} The fraction of the excited electron distribution that is trapped into defects depends on the level of compensation of the $A_{S_{Ga}}$ band and the optically injected carrier density.⁴⁵ Recombination of trapped

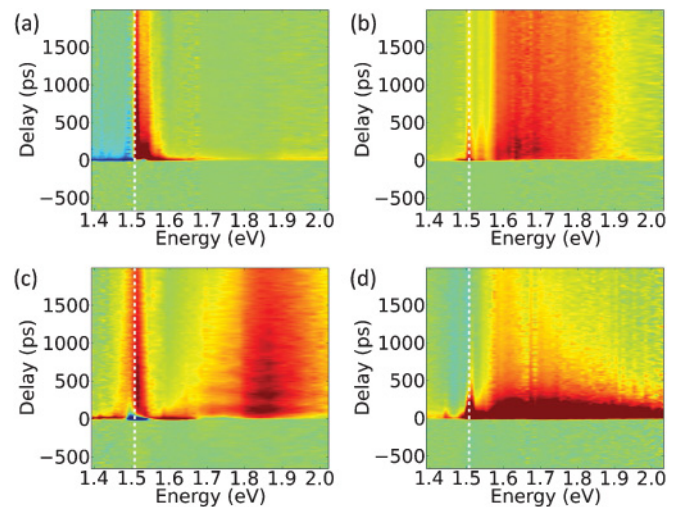


FIG. 2. (Color online) Results of spectrally resolved differential reflectivity experiments on (a) SI GaAs, (b) GaMnAs (150 nm thickness) (c) LT-GaAs and (d) GaMnAs (20 nm thickness). The band gap of SI-GaAs at 80 K (1.507 eV) is indicated by a vertical dashed line. The contour scale indicates the size (and sign) of $\Delta R/R_0$, which extends from -1.0% to $+1.0\%$ in (a) and from -0.4% to 0.4% in (b)–(d). $\Delta R/R_0$ is positive (dark grey, red online) or zero (light grey, green online), except for a rapid negative response (black, blue online) below 1.507 eV in (a) and around 1.507 eV in (c).

electrons with valence-band holes occurs on a nanosecond time scale.⁴⁶ Excited carriers in band states lead to reduced absorption due to the Pauli exclusion principle (state filling, SF) and increased absorption through intraband excitation (free-carrier absorption, FCA). A transient red shift of the band gap associated with the exchange interaction among the optically excited electrons and holes will also modify the optical response of the probe beam (band-gap renormalization, BGR). Electrons that are trapped to mid-gap defect states will cause an increase in absorption through promotion of trapped electrons to states high in the conduction band (defect-induced absorption, DIA). As shown in Fig. 1(c), SF and BGR lead to dispersive signatures in the vicinity of the band gap, whereas FCA and DIA each contribute to a broadband optical response with opposite sign.

Comparison of the measured differential reflectivity response in SI-GaAs in Fig. 2(a) with the calculated curves in Fig. 1(c) suggests that it is dominated by a SF response, consistent with the findings in Ref. 48. A negative $\Delta R/R_0$ signal below the band gap is evident in the data in Fig. 2(a) for early time delays, attributed to FCA associated with the hot carrier distribution. Signatures of carrier thermalization, cooling, and recombination are seen in the observed dynamics in Figs. 1(b) and 2(a) for SI-GaAs, consistent with earlier studies.^{48–51} The appearance of a sharp onset of the $\Delta R/R_0$ response in the spectrally resolved results in Fig. 2(b) is in stark contrast to the results of linear-optical experiments on GaMnAs, in which strong band-tailing contributions dominate the optical response in the vicinity of the band edge. The observation of a clear edge in the nonlinear $\Delta R/R_0$ signal likely reflects the fact that band-tailing contributions are harder to saturate (i.e., it is more difficult to generate a SF response on the associated optical transitions) than the

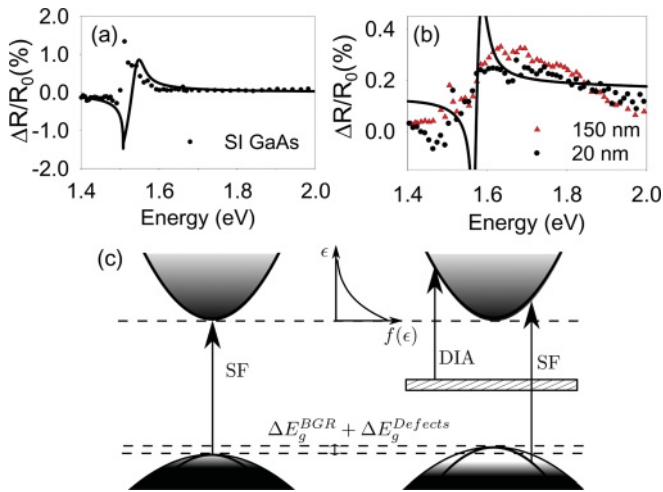


FIG. 3. (Color online) The differential reflectivity response at a probe pulse delay of 500 ps is shown for (a) SI-GaAs (circles) and (b) the two GaMnAs samples (150 nm thickness, triangles; 20 nm thickness, circles). The calculated differential reflectivity signals are also shown (solid curves), where (a) the full optically injected carrier density is included, and the $\Delta R/R_0$ includes only SF; and (b) the fraction of carriers trapped into the As_{Ga} band is 95%, and SF, DIA, and FCA were included. For the calculated curve in (b), the magnitude of the FCA contribution has been enhanced to account for the influence of defects, and the Moss-Burstein effect has been approximated by a rigid shift of the band gap of 55 meV. (c) Contributions to the $\Delta R/R_0$ response for SI-GaAs (left) and p-type LT-GaAs (right). The arrows indicate optical transitions induced by the probe pulse following excitation by the pump.

interband transitions.³⁷ We attribute the results in Fig. 2(b) to the combined effects of the portion of the electron distribution that is trapped into defect states within the first few picoseconds (leading to a broadband DIA response) and the remaining electrons in the conduction band, which lead to a SF signal and an associated sharp onset in the $\Delta R/R_0$ response in Fig. 2(b). This interpretation is supported by a comparison of the measured differential reflection spectrum at a probe-pulse delay of 500 ps with model calculations in which 95% of the electrons are assumed to be trapped to the As_{Ga} band [Fig. 3(b)]. The blue shift in the state-filling response of 55 meV relative to SI-GaAs is attributed to the presence of Mn, and is discussed further below. In Fig. 1(b), the negative signal around zero delay in the results for the GaMnAs sample is due to FCA, which is enhanced with low-temperature growth due to the presence of defects.^{41,42,47,52} The subsequent rise, which is characterized by a time constant of 1.8 ps, is attributed to the trapping of a portion of the electrons into As_{Ga} defects, after which a positive signal is observed due to a DIA response associated with the trapped carriers.

The weak feature at the band gap of SI-GaAs (1.507 eV) in the results for GaMnAs in Fig. 2(b) is attributed to the optical response of the GaAs buffer layer, which is expected to exhibit a similar spectral response to the SI-GaAs sample since it is grown at high substrate temperature. This assignment was confirmed through comparison to measurements on the 20-nm GaMnAs sample [Fig. 2(d)], which exhibits similar characteristics, including a broad response with a sharp onset

at ~ 1.56 eV and a feature at 1.507 eV. The larger size of the signal at 1.507 eV in the 20-nm sample relative to the 150-nm sample confirms its identification as an optical response of the buffer layer. Weak oscillations are also observed in both GaMnAs samples, with a period of a few tens of picoseconds, attributed to the excitation of coherent phonons in the surface layer.^{8,40} The weak feature around 1.55 eV in the 150-nm GaMnAs sample is not present in the 20-nm sample. The origin of this small signal is not known.

Results of $\Delta R/R_0$ measurements in the LT-GaAs sample are shown in Fig. 2(c). A spectrally broad feature associated with DIA is also observed in this sample associated with the As_{Ga} defects introduced during low-temperature growth. The magnitude and shape of the DIA signal differs in each of the three low-temperature-grown samples. Variations in the density of defects and the level of compensation will affect the initial density of trapping sites,⁴⁵ and changes in the nature of disorder will modify the density of states high in the conduction band,³⁴ representing possible sources of variation in the DIA response among the samples. The DIA signal also exhibits a faster rate of decay in the 20-nm GaMnAs sample and the LT-GaAs sample than in the 150-nm GaMnAs sample, implying a faster recombination rate from trap states.⁴⁶ The most notable difference between the $\Delta R/R_0$ response for LT-GaAs and GaMnAs is the spectral position of the SF signal due to the residual carriers in the conduction band following the trapping process: In LT-GaAs this SF response occurs *below* the band gap of SI-GaAs, whereas in GaMnAs it occurs above the band gap. The blue shift in the SF response in GaMnAs is tied to the incorporation of Mn.

As discussed above, an active debate in the recent literature has focused on the position of the Fermi level in GaMnAs, which may lie in the valence band or in an impurity band. As this issue has crucial implications regarding the nature of hole transport and the mechanism of ferromagnetic coupling, it is essential that it be resolved in order that a broad understanding of the properties of DMS materials may be developed. Linear absorption experiments at the fundamental band gap do not address this issue because the band-gap energy is not observable due to strong contributions to the absorption from band-tailing effects.^{17,34–36} Furthermore, measurements using other linear-optical techniques (magnetic circular dichroism, midinfrared absorption) have yielded conflicting results.^{16,18,20,34} In heavily doped p-type semiconductors, the Fermi level resides below the edge of the valence band, implying that the energetic onset for linear absorption will occur at higher energies than in the corresponding undoped semiconductor. This blue shift in the linear absorption response due to filling of the valence-band states by doped carriers is known as the Moss-Burstein shift.³² Assuming the holes in GaMnAs reside in the valence band, a rough estimate of the magnitude of the Moss-Burstein shift is provided by a calculation of the Fermi energy in the valence band.⁵³ Coupling of carriers in the band states with impurities leads to an upward shift of the valence-band edge, resulting in a reduction of the band gap. BGR associated with the high density of holes present due to doping will also lead to a reduction in the band-gap energy. The calculated results for both of these effects were taken from Ref. 53, and are summarized in Table I. Only the net trend is meaningful for the total band-gap shift, since the magnitude of the red shifts

TABLE I. Estimated changes (in meV) of the band gap expected for p-type, low-temperature-grown GaAs as a function of hole density p (in cm^{-3}). The first column contains the approximate Fermi energy in the valence band within an effective mass model. Data for the second and third columns were adapted from Ref. 53.

p	Hole E_F	ΔE_g^{BGR}	$\Delta E_g^{\text{Defects}}$	$\Delta E_g^{\text{Total}}$
1×10^{19}	33	-39	-8	-14
5×10^{19}	96	-52	-21	23
1×10^{20}	157	-72	-29	56
5×10^{20}	459	-140	-90	229
1×10^{21}	729	-170	-143	416

are very sensitive to the defect distribution.⁵³ Nevertheless, the observation of a blue shift is consistent with the occupation of states in the valence band with holes. In contrast, if holes *only* reside in an impurity band (regardless of its energetic position relative to the valence-band edge), the Moss-Burstein effect would be absent, and a red shift of the band gap is expected as only the defect-induced renormalization would occur, in agreement with the $\Delta R/R_0$ response in LT-GaAs. The observation of a blue shift in the onset of the differential reflectivity response of GaMnAs relative to that in SI-GaAs therefore supports the valence-band picture of ferromagnetism in this material. The magnitude of blue shift (~ 55 meV) was observed to be equal within the experimental uncertainty (9 meV, dictated by the monochromator resolution) in the two GaMnAs samples studied here, which are expected to have similar hole concentrations,^{16,54} lending support to this conclusion.

It should be noted that optical transitions between the band states and the Mn_{Ga} impurity level have been shown to produce strong contributions in magnetic circular dichroism

experiments.^{19,20} In an impurity band description of ferromagnetism, a differential reflectivity signal may be expected associated with optically injected holes that relax into the impurity band states. For transitions from the Mn_{Ga} level to the conduction band, the associated process would lead to a state-filling response (i.e., absorption bleaching) below the band gap,³³ in contrast to the blue-shifted response we observe here. For transitions from deep in the valence band to the Mn_{Ga} impurity level, increased absorption would contribute to a $\Delta R/R_0$ response. Such a signal is expected to extend over a broad energy range (covering energies above and below E_g).^{19,20} It is not clear how such a broad signal could lead to a sharp edge above the band gap of GaAs. More theoretical work is needed to investigate the possible role of transitions between Mn_{Ga} impurity states and the band states in nonlinear optical experiments, such as those reported here.

In summary, spectrally and temporally resolved differential reflectivity experiments on GaMnAs indicate a sharp band-edge response, a feature that is tied to a reduction in the relative importance of band-tail contributions in nonlinear optical experiments. As no band gap could be identified in earlier studies on GaMnAs using linear spectroscopy, our observations illustrate the power of nonlinear pump-probe techniques for studying the electronic structure of GaMnAs. The observation of a blue shift in the band-edge response in GaMnAs is interpreted in terms of the valence-band model of ferromagnetism.

This research is supported by the Canada Foundation for Innovation, the Natural Sciences and Engineering Research Council of Canada, Lockheed Martin Corporation, the Canada Research Chairs Program, and the Czech Republic Grants No. LC510 and No. KAN400100652.

¹*Semiconductor Spintronics and Quantum Computation*, edited by D. D. Awschalom, D. Loss, and N. Samarth (Springer-Verlag, Berlin, 2002).

²K. C. Hall, W. H. Lau, K. Gündoğdu, M. E. Flatté, and T. F. Bogge, *Appl. Phys. Lett.* **83**, 2937 (2003).

³K. C. Hall and M. E. Flatté, *Appl. Phys. Lett.* **88**, 162503 (2006).

⁴T. Kuroiwa, T. Yasuda, F. Matsukura, A. Shen, Y. Ohno, Y. Segawa, and H. Ohno, *Electron. Lett.* **34**, 190 (1998).

⁵K. Onodera, T. Masumoto, and M. Kimura, *Electron. Lett.* **30**, 1954 (1994).

⁶J. Rudolph, D. Hägele, H. M. Gibbs, G. Khitrova, and M. Oestreich, *Appl. Phys. Lett.* **82**, 4516 (2003).

⁷K. C. Hall, J. P. Zahn, A. Gamouras, S. March, J. L. Robb, X. Liu, and J. K. Furdyna, *Appl. Phys. Lett.* **93**, 032504 (2008).

⁸J. P. Zahn, A. Gamouras, S. March, X. Liu, J. K. Furdyna, and K. C. Hall, *J. Appl. Phys.* **107**, 033908 (2010).

⁹A. H. M. Reid, G. V. Astakhov, A. V. Kimel, G. M. Schott, W. Ossau, K. Brunner, A. Kirilyuk, L. W. Molenkamp, and Th. Rasing, *Appl. Phys. Lett.* **97**, 232503 (2010).

¹⁰H. Ohno, D. Chiba, F. Matsukura, T. Omiya, E. Abe, T. Dietl, Y. Ohno, and K. Ohtani, *Nature (London)* **408**, 944 (2000).

¹¹D. Chiba, M. Yamanouchi, F. Matsukura, and H. Ohno, *Science* **301**, 943 (2003).

¹²S. Koshihara, A. Oiwa, M. Hirasawa, S. Katsumoto, Y. Iye, C. Urano, H. Takagi, and H. Munekata, *Phys. Rev. Lett.* **78**, 4617 (1997).

¹³A. Oiwa, T. Slupinski, and H. Munekata, *Appl. Phys. Lett.* **78**, 518 (2001).

¹⁴V. Novák, K. Olejník, J. Wunderlich, M. Cukr, K. Výborný, A. W. Rushforth, K. W. Edmonds, R. P. Campion, B. L. Gallagher, Jairo Sinova, and T. Jungwirth, *Phys. Rev. Lett.* **101**, 077201 (2008).

¹⁵P. Vašek, P. Svoboda, V. Novák, M. Cukr, Z. Výborný, V. Jurka, J. Stuchlík, M. Orlita, and D. K. Maude, *J. Supercond. Novel Magn.* **23**, 1161 (2010).

¹⁶T. Jungwirth, P. Horodyská, N. Tesařová, P. Němec, J. Šubrt, P. Malý, P. Kužel, C. Kadlec, J. Masek, I. Němec, M. Orlita, V. Novák, K. Olejník, Z. Šobáň, P. Vašek, P. Svoboda, and J. Sinova, *Phys. Rev. Lett.* **105**, 227201 (2010); see also supplementary material.

¹⁷J. Szczytko, W. Mac, A. Twardowski, F. Matsukura, and H. Ohno, *Phys. Rev. B* **59**, 12935 (1999).

¹⁸B. Beschoten, P. A. Crowell, I. Malajovich, D. D. Awschalom, F. Matsukura, A. Shen, and H. Ohno, *Phys. Rev. Lett.* **83**, 3073 (1999).

¹⁹J.-M. Tang and M. E. Flatté, *Phys. Rev. Lett.* **101**, 157203 (2008).

- ²⁰K. Ando, H. Saito, K. C. Agarwal, M. C. Debnath, and V. Zayets, *Phys. Rev. Lett.* **100**, 067204 (2008).
- ²¹G. Acbas, M.-H. Kim, M. Cukr, V. Novák, M. A. Scarpulla, O. D. Dubon, T. Jungwirth, Jairo Sinova, and J. Cerne, *Phys. Rev. Lett.* **103**, 137201 (2009).
- ²²K.-Y. Wang, M. Sawicki, K. W. Edmonds, R. P. Campion, S. Maat, C. T. Foxon, B. L. Gallagher, and T. Dietl, *Phys. Rev. Lett.* **95**, 217204 (2005).
- ²³L. V. Titova, M. Kutrowski, X. Liu, R. Chakarvorty, W. L. Lim, T. Wojtowicz, J. K. Furdyna, and M. Dobrowolska, *Phys. Rev. B* **72**, 165205 (2005).
- ²⁴M. Abolfath, T. Jungwirth, J. Brum, and A. H. MacDonald, *Phys. Rev. B* **63**, 054418 (2001).
- ²⁵T. Dietl, J. König, and A. H. MacDonald, *Phys. Rev. B* **64**, 241201(R) (2001).
- ²⁶A. H. MacDonald, P. Schiffer, and N. Samarth, *Nature Mater.* **4**, 195 (2005).
- ²⁷K. S. Burch, D. B. Shrekenhamer, E. J. Singley, J. Stephens, B. L. Sheu, R. K. Kawakami, P. Schiffer, N. Samarth, D. D. Awschalom, and D. N. Basov, *Phys. Rev. Lett.* **97**, 087208 (2006).
- ²⁸B. L. Sheu, R. C. Myers, J.-M. Tang, N. Samarth, D. D. Awschalom, P. Schiffer, and M. E. Flatté, *Phys. Rev. Lett.* **99**, 227205 (2007).
- ²⁹S. Ohya, K. Takata, and M. Tanaka, *Nature Phys.* **7**, 342 (2011).
- ³⁰E. J. Singley, K. S. Burch, R. Kawakami, J. Stephens, D. D. Awschalom, and D. N. Basov, *Phys. Rev. B* **68**, 165204 (2003).
- ³¹T. Dietl, H. Ohno, and F. Matsukura, *Phys. Rev. B* **63**, 195205 (2001).
- ³²T. S. Moss, *Proc. Phys. Soc. B* **67**, 775 (1954); E. Burstein, *Phys. Rev.* **93**, 632 (1954).
- ³³A. Lohner, M. Woerner, T. Elsaesser, and W. Kaiser, *Phys. Rev. Lett.* **68**, 3920 (1992).
- ³⁴K. S. Burch, J. Stephens, R. K. Kawakami, D. D. Awschalom, and D. N. Basov, *Phys. Rev. B* **70**, 205208 (2004).
- ³⁵D. Streb, M. Ruff, S. U. Dankowski, P. Kiesel, M. Kneissl, S. Malzer, U. D. Keil, and G. H. Döhler, *J. Vac. Sci. Technol. B* **14**, 2275 (1996).
- ³⁶Sajeev John, Costas Soukoulis, Morrel H. Cohen, and E. N. Economou, *Phys. Rev. Lett.* **57**, 1777 (1986).
- ³⁷M. Haiml, U. Siegner, F. Morier-Genoud, U. Keller, M. Luysberg, R. C. Lutz, P. Specht, and E. R. Weber, *Appl. Phys. Lett.* **74**, 3134 (1999).
- ³⁸D. C. Hutchings, M. Sheik-Bahae, D. J. Hagan, and E. W. Van Stryland, *Opt. Quantum Electron.* **24**, 1 (1992).
- ³⁹J. Shah, *Ultrafast Spectroscopy of Semiconductors and Semiconductor Nanostructures* (Springer-Verlag, Berlin, 1996).
- ⁴⁰J. Wang, Y. Hashimoto, J. Kono, A. Oiwa, H. Munekeata, G. D. Sanders, and C. J. Stanton, *Phys. Rev. B* **72**, 153311 (2005).
- ⁴¹K. J. Yee, D. Lee, X. Liu, W. L. Lim, M. Dobrowolska, J. K. Furdyna, Y. S. Lim, K. G. Lee, Y. H. Ahn, and D. S. Kim, *J. Appl. Phys.* **98**, 113509 (2005).
- ⁴²S. Kim, E. Oh, J. U. Lee, D. S. Kim, S. Lee, and J. K. Furdyna, *Appl. Phys. Lett.* **88**, 262101 (2006).
- ⁴³J.-H. Kim, K.-J. Han, D.-W. Jang, K.-J. Yee, X. Liu, and J. K. Furdyna, *J. Korean Phys. Soc.* **50**, 819 (2007).
- ⁴⁴E. Rozkotová, P. Němec, D. Sprinzl, P. Horodyská, F. Trojánek, P. Malý, V. Novák, K. Olejník, M. Cukr, and T. Jungwirth, *IEEE Trans. Magn.* **44**, 2674 (2008).
- ⁴⁵H. S. Loka, S. D. Benjamin, and P. W. E. Smith, *IEEE J. Quant. Electron.* **34**, 1426 (1998).
- ⁴⁶A. J. Lochtefeld, M. R. Melloch, J. C. P. Chang, and E. S. Harmon, *Appl. Phys. Lett.* **69**, 1465 (1996).
- ⁴⁷S. Gupta, M. Y. Frankel, J. A. Valdmanis, J. F. Whitaker, G. A. Mourou, F. W. Smith, and A. R. Calawa, *Appl. Phys. Lett.* **59**, 3276 (1991).
- ⁴⁸Y. H. Lee, A. Chavez-Pirson, S. W. Koch, H. M. Gibbs, S. H. Park, J. Morhange, A. Jeffery, N. Peyghambarian, L. Banyai, A. C. Gossard, and W. Wiegmann, *Phys. Rev. Lett.* **57**, 2446 (1986).
- ⁴⁹J. Kunde, S. Arlt, L. Gallmann, F. Morier-Genoud, U. Seigner, and U. Keller, *J. Appl. Phys.* **88**, 1187 (2000).
- ⁵⁰A. Alexandrou, V. Berger, and D. Hulin, *Phys. Rev. B* **52**, 4654 (1995).
- ⁵¹S. Hunsche, H. Heesel, A. Ewertz, H. Kurz, and J. H. Collet, *Phys. Rev. B* **48**, 17818 (1993).
- ⁵²J. Kuhl, E. O. Göbel, Th. Pfeiffer, and A. Jonietz, *Appl. Phys. A* **34**, 105 (1984).
- ⁵³Y. Zhang and S. Das Sarma, *Phys. Rev. B* **72**, 125303 (2005).
- ⁵⁴Similar blue shifts may still be expected for the two GaMnAs samples despite small differences in hole concentration due to differing defect distributions for samples with different layer thicknesses (Ref. 16). For example, an increased prevalence of impurity complexes would reduce $\Delta E_g^{\text{Defects}}$, as discussed in Ref. 53.